

# Observational constraint on dynamical evolution of dark energy

Yungui Gong\*

*College of Mathematics and Physics,*

*Chongqing University of Posts and Telecommunications, Chongqing 400065, China*

Rong-Gen Cai<sup>†</sup>

*Institute of Theoretical Physics, Chinese Academy*

*of Sciences, Beijing 100190, P. R. China and*

*College of Mathematics and Physics,*

*Chongqing University of Posts and Telecommunications, Chongqing 400065, China*

Yun Chen, Zong-Hong Zhu<sup>‡</sup>

*Department of Astronomy, Beijing Normal University, Beijing 100875, China*

## Abstract

We use the Constitution supernova, the baryon acoustic oscillation, the cosmic microwave background, and the Hubble parameter data to analyze the evolution property of dark energy. We obtain different results when we fit different baryon acoustic oscillation data combined with the Constitution supernova data to the Chevallier-Polarski-Linder model. We find that the difference stems from the different values of  $\Omega_{m0}$ . We also fit the observational data to the model independent piecewise constant parametrization. Four redshift bins with boundaries at  $z = 0.22, 0.53, 0.85$  and  $1.8$  were chosen for the piecewise constant parametrization of the equation of state parameter  $w(z)$  of dark energy. We find no significant evidence for evolving  $w(z)$ . With the addition of the Hubble parameter, the constraint on the equation of state parameter at high redshift is improved by 70%. The marginalization of the nuisance parameter connected to the supernova distance modulus is discussed.

PACS numbers: 95.36.+x, 98.80.Es

---

\*Electronic address: gongyg@cqupt.edu.cn

<sup>†</sup>Electronic address: cairg@itp.ac.cn

<sup>‡</sup>Electronic address: zhuzh@bnu.edu.cn

## I. INTRODUCTION

Since the discovery of the late time cosmic acceleration by the Type Ia supernova (SnIa) observations [1, 2], a lot of efforts have been made to understand the driving force behind the cosmic acceleration. The standard models in cosmology and particle physics give no answer to this problem. To address the problem, one needs to modify either the left hand side or the right hand side of Einstein equation. Modifying the left hand side means that general relativity is modified, models such as the Dvali-Gabadadze-Porrati model [3], and  $f(R)$  gravity [4–13], have been proposed along this line of reasoning. On the other hand, in the framework of Einstein gravity, an exotic form of matter with negative pressure, dubbed as dark energy, has to be introduced into the right hand side of Einstein equation to explain the phenomenon of cosmic acceleration. However, the nature and origin of dark energy remain a mystery. Many parametric and nonparametric model-independent methods were proposed to study the property of dark energy, see for example [14–34] and references therein.

Recently, it was claimed that the flat  $\Lambda$ CDM model is inconsistent with the current data at more than  $1\sigma$  level [35–38]. Furthermore, it was suggested that the cosmic acceleration is slowing down from  $z \sim 0.3$  in [35]. The analysis in [35] is based on the commonly used Chevallier-Polarski-Linder (CPL) model [33, 34] with the Constitution SnIa [39] and the baryon acoustic oscillation (BAO) distance ratio data [40], the result is somewhat model dependent. In [36], the authors applied the Union SnIa data [41], together with the BAO  $A$  parameter [42] and gamma-ray bursts data to the piecewise constant parametrization of the equation of state parameter of dark energy. In this analysis, the equation of state parameter  $w$  of dark energy is a constant in a redshift bin, and three redshift bins with boundaries at  $z = 0.2, 0.5$  and  $1.0$  were chosen. They also analyzed the Constitution SnIa and the BAO distance ratio data. In [37], the authors considered two redshift bins by using the Constitution SnIa data, and they found that dark energy suddenly emerged at redshift  $z \sim 0.3$ . The results obtained in [38] were based on the analysis of the Constitution SnIa, the full Wilkinson microwave anisotropy probe 5 year (WMAP5) [43] and the Sloan digital sky survey (SDSS) data. For the redshift range  $0 \leq z \leq 1$ , four evenly spaced redshift bins were chosen. However, choosing the same four evenly spaced redshift bins, the authors in [44] found no evidence for dark energy dynamics by using the Constitution SnIa, WMAP5, BAO [45], the integrated Sachs-Wolfe effect, galaxy clustering and weak lensing

data. Different data sets and analysis may give different results. In this paper, we apply the piecewise constant parametrization of the equation of state parameter  $w(z)$  to do a more careful model independent analysis. We choose four redshift bins by requiring  $N\Delta z \sim 30$  in each bin, and we use the Constitution SnIa [39], the BAO [40], the derived WMAP5 [43] and the Hubble parameter  $H(z)$  data [46–48].

This paper is organized as follows. In section II, we first review the analysis by using the CPL model in [35], and find that their result heavily depends on the choice of BAO data. By using the BAO distance ratio data, the best fit value of  $\Omega_{m0} = 0.45_{-0.11}^{+0.07}$ , which is not consistent with other observational result. On the other hand, the best fit value of  $\Omega_{m0} = 0.29_{-0.04}^{+0.05}$  if the BAO  $A$  parameter is used. Then we apply the SnIa, BAO, WMAP5 and  $H(z)$  data to study the property of dark energy by using the piecewise constant parametrization of the equation of state parameter  $w(z)$ , in section III. We conclude the paper in section IV.

## II. OBSERVATIONAL CONSTRAINTS ON CPL PARAMETRIZATION

To study the dynamical property of dark energy by observational data, one usually parameterizes the equation of state parameter  $w(z)$ . Following [35], we first study the CPL parametrization

$$w(z) = w_0 + \frac{w_a z}{1+z}. \quad (1)$$

The dimensionless Hubble parameter for a flat universe is

$$E^2(z) = \frac{H^2(z)}{H_0^2} = \Omega_{m0}(1+z)^3 + (1-\Omega_{m0})(1+z)^{3(1+w_0+w_a)} \exp(-3w_a z/(1+z)). \quad (2)$$

In this model, we have three parameters  $\Omega_{m0}$ ,  $w_0$  and  $w_a$ , let us denote them as  $\mathbf{p} = (\Omega_{m0}, w_0, w_a)$ . We first use the Constitution compilation of 397 SnIa data [39] to constrain the model parameters  $\mathbf{p}$ . The Constitution sample adds 185 CfA3 SnIa data to the Union sample [41]. The addition of CfA3 sample increases the number of nearby SnIa by a factor of roughly 2.6 – 2.9 and reduces the statistical uncertainties. The Union compilation has 57 nearby SnIa and 250 high- $z$  SnIa. It includes the Supernova Legacy Survey [49] and the ESSENCE Survey [50, 51], the older observed SnIa data, and the extended data set of

distant SnIa observed with the Hubble space telescope. To fit the SnIa data, we define

$$\chi_{sn}^2(\mathbf{p}, H_0^n) = \sum_{i=1}^{397} \frac{[\mu_{obs}(z_i) - \mu(z_i, \mathbf{p}, H_0^n)]^2}{\sigma_i^2}, \quad (3)$$

where the extinction-corrected distance modulus  $\mu(z)$  is the difference between the apparent magnitude  $m(z)$  and the absolute magnitude  $M$  of a supernova at redshift  $z$ ,

$$\mu(z, \mathbf{p}, H_0^n) = m(z) - M = 25 - 5 \log_{10} H_0^n + 5 \log_{10}[D_L(z)/\text{Mpc}],$$

the absolute magnitude  $M$  applies equally to all magnitude measurement, and its effect is manifested by the nuisance parameter  $H_0^n$ ;  $\sigma_i$  is the total uncertainty which includes the intrinsic uncertainty of 0.138 mag for each CfA3 SnIa, the peculiar velocity uncertainty of 400km/s, and the redshift uncertainty [39]; and the Hubble constant free luminosity distance  $D_L(z) = H_0 d_L(z)$  is

$$D_L(z, \mathbf{p}) = H_0 d_L(z) = \frac{1+z}{\sqrt{|\Omega_k|}} \text{sinn} \left[ \sqrt{|\Omega_k|} \int_0^z \frac{dx}{E(x, \mathbf{p})} \right], \quad (4)$$

where

$$\frac{\text{sinn}(\sqrt{|\Omega_k|x})}{\sqrt{|\Omega_k|}} = \begin{cases} \sin(\sqrt{|\Omega_k|x})/\sqrt{|\Omega_k|}, & \text{if } \Omega_k < 0, \\ x, & \text{if } \Omega_k = 0, \\ \sinh(\sqrt{|\Omega_k|x})/\sqrt{|\Omega_k|}, & \text{if } \Omega_k > 0. \end{cases} \quad (5)$$

The nuisance parameter  $H_0^n$  is marginalized over with a flat prior when we apply the SnIa data. For the details of the marginalization method, see [26, 27]. Then we add the BAO parameter  $A = 0.469(0.96/0.98)^{-0.35} \pm 0.017$  [42] into the SnIa data to determine the parameters  $\mathbf{p}$ . So we have  $\chi^2(\mathbf{p}) = [A - 0.469(0.96/0.98)^{-0.35}]^2/0.017^2 + \chi_{sn}^2$ . The BAO parameter  $A$  in a spatially flat universe is defined as

$$A(\mathbf{p}) = \sqrt{\Omega_{m0}} \frac{H_0 D_V(z_{bao}, \mathbf{p}, H_0)}{z_{bao}} = \frac{\sqrt{\Omega_{m0}}}{z_{bao}} \left[ \frac{z_{bao}}{E(z_{bao})} \left( \int_0^{z_{bao}} \frac{dz}{E(z)} \right)^2 \right]^{1/3}, \quad (6)$$

where  $z_{bao} = 0.35$ , and the effective distance

$$D_V(z, \mathbf{p}, H_0) = \frac{1}{H_0} \left[ \frac{D_L^2(z)}{(1+z)^2} \frac{z}{E(z)} \right]^{1/3}. \quad (7)$$

Finally we add the shift parameter  $R$  with which the  $l$ -space positions of the acoustic peaks in the angular power spectrum shift, to the combined SnIa and BAO  $A$  data. The shift parameter

$$R(\mathbf{p}) = \sqrt{\Omega_{m0}} \int_0^{z_{ls}} \frac{dz}{E(z)} = 1.710 \pm 0.019, \quad (8)$$

where the last scattering surface redshift  $z_{ls} = 1090.0$ . So now we minimize

$$\chi^2(\mathbf{p}) = \frac{(R - 1.71)^2}{0.019^2} + \frac{[A - 0.469(0.96/0.98)^{-0.35}]^2}{0.017^2} + \chi_{sn}^2.$$

Fitting the Constitution SnIa data, the BAO distance ratio  $D_V(z = 0.35)/D_V(z = 0.20) = 1.736 \pm 0.065$  (hereafter BAO I) [45] and the shift parameter  $R$  to the CPL model, the authors in [35] conclude that the functional form of the CPL ansatz is unable to fit the data simultaneously at low and high redshifts. In this section, we replace the BAO distance ratio data (BAO I) by the BAO parameter  $A$  (hereafter BAO II) to fit the CPL model. By fitting the SnIa, SnIa+BAO I (II), and the SnIa+BAO I (II)+ $R$  data to the CPL model, we obtain the joint constraints on the parameters  $\Omega_{m0}$ ,  $w_0$  and  $w_a$  in the CPL model. The values of  $\Omega_{m0}$  and  $\chi^2$  constrained from different data sets are shown in Table I. For the purpose of comparing the results, we only show the constraint on  $\Omega_{m0}$  in Table I. For the SnIa+BAO I data, the joint  $1\sigma$  constraints are  $\Omega_{m0} = 0.45_{-0.11}^{+0.07}$ ,  $w_0 = -0.13_{-0.95}^{+1.26}$  and  $w_a = -12.2_{-15.3}^{+10.3}$ . Fitting the SnIa+BAO II data to the CPL model, the joint  $1\sigma$  constraints are  $\Omega_{m0} = 0.29_{-0.04}^{+0.05}$ ,  $w_0 = -0.90_{-0.37}^{+0.46}$  and  $w_a = -0.6_{-3.5}^{+2.5}$ . Comparing these results, we find that  $w_0$  and  $w_a$  are consistent with each other at  $1\sigma$  level, but  $\Omega_{m0}$  is barely consistent with each other at  $1\sigma$  level. For the SnIa data or the SnIa+BAO I data, the best fit value of  $\Omega_{m0}$  is much larger than the value  $\Omega_{m0} \sim 0.3$  obtained from other observational constraint, and that makes the result inconsistent with the  $\Lambda$ CDM model at more than  $1\sigma$  level. The BAO II data or the WMAP5 data lowers the value of  $\Omega_{m0}$ , and therefore makes the result consistent with the  $\Lambda$ CDM model at  $1\sigma$  level. To compare our results with those in [35],

Data	CPL model	$\Lambda$ CDM model
SnIa	$\Omega_{m0} = 0.45_{-0.13}^{+0.07}$ , $\chi^2 = 462.07$	$\Omega_{m0} = 0.29 \pm 0.02$ , $\chi^2 = 466.32$
SnIa + BAO I	$\Omega_{m0} = 0.45_{-0.11}^{+0.07}$ , $\chi^2 = 462.44$	$\Omega_{m0} = 0.29 \pm 0.02$ , $\chi^2 = 467.61$
SnIa + BAO II	$\Omega_{m0} = 0.29_{-0.04}^{+0.05}$ , $\chi^2 = 466.18$	$\Omega_{m0} = 0.28 \pm 0.02$ , $\chi^2 = 466.42$
SnIa + BAO I + $R$	$\Omega_{m0} = 0.26_{-0.04}^{+0.08}$ , $\chi^2 = 467.74$	$\Omega_{m0} = 0.27 \pm 0.02$ , $\chi^2 = 469.49$
SnIa + BAO II + $R$	$\Omega_{m0} = 0.27 \pm 0.03$ , $\chi^2 = 466.81$	$\Omega_{m0} = 0.27 \pm 0.01$ , $\chi^2 = 468.42$

TABLE I: The  $1\sigma$  error estimate of  $\Omega_{m0}$  for the CPL model and  $\Lambda$ CDM model.

we also show the evolutions of  $q(z)$  and  $Om(z)$  constrained from SnIa, SnIa+BAO II and

SnIa+BAO II+ $R$  in Fig. 1. The deceleration parameter

$$q(z) = \frac{\Omega_{m0}(1+z)^3 + [1 + 3w(z)](1 - \Omega_{m0})(1+z)^{3(1+w_0+w_a)} \exp(-3w_a z/(1+z))}{2E^2(z)}, \quad (9)$$

and  $Om(z)$  is defined as

$$Om(z) = \frac{E^2(z) - 1}{(1+z)^3 - 1}. \quad (10)$$

The evolution of  $q(z)$  gives us the information about how fast the Universe expands. The sign of  $q(z)$  shows whether the expansion is accelerating or decelerating,  $q(z) > 0$  means deceleration. For a  $\Lambda$ CDM model,  $Om(z) = \Omega_{m0}$  is a constant. Also at low redshift, larger  $Om(z)$  means larger  $w$  of dark energy.

Comparing the evolutions of  $q(z)$  and  $Om(z)$  shown in our Fig. 1 with those in the Fig. 2 of [35], we find that the value of  $\Omega_{m0}$  constrained from the sample is the main reason of different evolutions of  $q(z)$  and  $Om(z)$ . Because of the relative large  $\Omega_{m0}$  obtained from SnIa + BAO I data, the result is inconsistent with  $\Lambda$ CDM model at more than  $1\sigma$  level. This can be easily understood by expanding  $Om(z)$  for the CPL model at low redshift,  $Om(z) \approx 1 + w_0(1 - \Omega_{m0})$ . Even if we get  $w_0$  close to  $-1$ , the large value of  $\Omega_{m0}$  will make the CPL model inconsistent with  $\Lambda$ CDM model. However, if we impose a prior on  $\Omega_{m0}$ , for example,  $\Omega_{m0} = 0.28 \pm 0.04$ , then the result by fitting the SnIa data or SnIa+BAO I data to the CPL model, is consistent with the  $\Lambda$ CDM model.

### III. OBSERVATIONAL CONSTRAINTS ON PIECEWISE CONSTANT PARAMETRIZATION

Although the CPL parametrization provides a useful tool to study the dynamical property of dark energy, the particular form of  $w(z)$  may impose a strong prior. Note that in a small enough redshift region,  $w(z)$  is approximately a constant, so we may divide the redshift into several bins, and parameterize  $w(z)$  as a constant in a particular redshift bin, this is the piecewise constant parametrization of  $w(z)$ . If we have enough data, the redshift range in each bin can be small enough, and the piecewise constant parametrization gives the true  $w(z)$ . In other words, the piecewise constant parametrization is a model independent method. In practice, the number of redshift bins is finite, and the piecewise constant parametrization of  $w$  is an approximation of the true  $w(z)$ , and it provides very useful information about the dynamical behavior of dark energy. In this section, we use

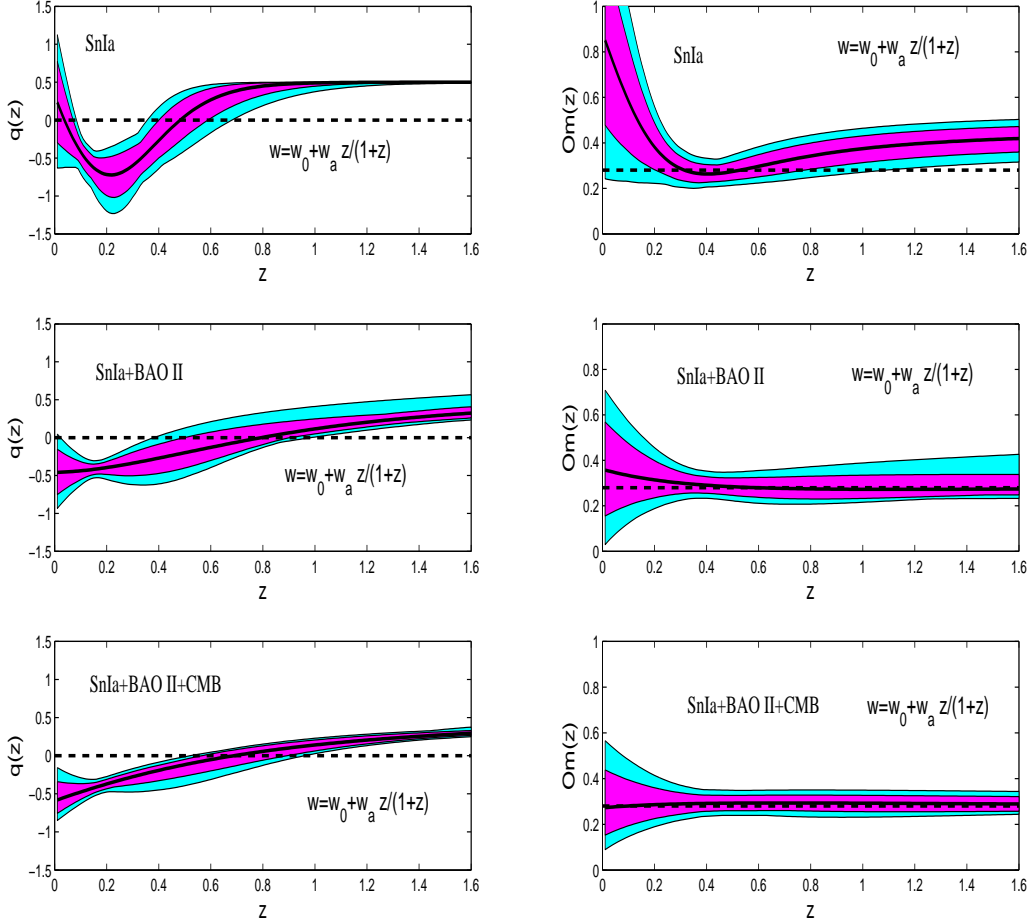


FIG. 1: Reconstructed  $q(z)$  and  $Om(z)$  from SnIa data, SnIa+BAO II data and SnIa+BAO II+CMB data using the CPL ansatz. The center solid lines are plotted with the best fit values, and the shadows denote the  $1\sigma$  and  $2\sigma$  limits. The spatially flat  $\Lambda$ CDM model corresponds to a horizontal dashed line with  $Om(z) = 0.28$  in the right panels.

observational data to fit the piecewise constant parametrization of  $w(z)$ . For the binning of the Constitution SnIa data [39], we apply the uniform, unbiased binning method [50]. We group the data into four bins so that the number of SnIa in each bin times the width of each bin is around 30, i.e.,  $N\Delta z \sim 30$ ,  $N$  is the number of SnIa in each bin,  $\Delta z$  is the width of each bin. The choice of  $N\Delta z \sim 30$  for the Constitution SnIa data results in four bins. The boundaries of the four bins are  $z_1 = 0.22$ ,  $z_2 = 0.53$ ,  $z_3 = 0.85$ ,  $z_4 = 1.8$  and  $z_5$  extends beyond 1089. For the redshift in the range  $z_{i-1} < z < z_i$ , the equation of state

parameter is a constant,  $w(z) = w_i$ . For convenience, we choose  $z_0 = 0$ . Due to the lack of observational data in the redshift range  $z = 1.8 - 1089$ ,  $w(z)$  is largely unconstrained in this redshift range. For simplicity, we assume that  $w(z > 1.8) = -1$ . For a flat universe, the Friedmann equation becomes

$$E^2(z) = \Omega_{m0}(1+z)^3 + (1-\Omega_{m0})(1+z)^{3(1+w_n)} \prod_{i=1}^n (1+z_{i-1})^{3(w_{i-1}-w_i)}, \quad z_{n-1} < z < z_n. \quad (11)$$

In this model, there are five free parameters  $\Omega_{m0}$ ,  $w_1$ ,  $w_2$ ,  $w_3$  and  $w_4$ , let us denote them as  $\boldsymbol{\theta} = (\Omega_{m0}, w_1, w_2, w_3, w_4)$ .

In general, the equation of state parameters  $w_i$  in different bins are correlated and their errors depend upon each other. We follow Huterer and Cooray [22] to transform the covariance matrix of  $w_i$  to decorrelate the error estimate. Explicitly, the transformation is

$$\mathcal{W}_i = \sum_j T_{ij} w_j, \quad (12)$$

where the transformation matrix  $T = V^T \Lambda^{-1/2} V$ , the orthogonal matrix  $V$  diagonalizes the covariance matrix  $C$  of  $w_i$  and  $\Lambda$  is the diagonalized matrix of  $C$ . For a given  $i$ ,  $T_{ij}$  can be thought of as weights for each  $w_j$  in the transformation from  $w_i$  to  $\mathcal{W}_i$ . We are free to rescale each  $\mathcal{W}_i$  without changing the diagonality of the correlation matrix, so we then multiply both sides of the equation above by an amount such that the sum of the weights  $\sum_j T_{ij}$  is equal to one. This allows for easy interpretation of the weights as a kind of discretized window function. Now the transformation matrix element is  $T_{ij}/\sum_k T_{ik}$  and the covariance matrix of the uncorrelated parameters is not the identity matrix. The  $i$ -th diagonal matrix element becomes  $(\sum_j T_{ij})^{-2}$ . In other words, the error of the uncorrelated parameters  $\mathcal{W}_i$  is  $\sigma_i = 1/\sum_j T_{ij}$ .

The likelihood for the parameters  $\boldsymbol{\theta}$  in the model and the nuisance parameters is computed using a Monte Carlo Markov Chain (MCMC). To observe the effect of the nuisance parameter  $H_0^n$  in the SnIa data, we take two different approaches. In the first approach, we analytically marginalize  $H_0^n$  by using a flat prior [27]. In the second approach, we take  $H_0^n = H_0$  as a free parameter in the MCMC code. The MCMC method randomly chooses values for the above parameters  $\boldsymbol{\theta}$ , evaluates  $\chi^2$  and determines whether to accept or reject the set of parameters  $\boldsymbol{\theta}$  using the Metropolis-Hastings algorithm. The set of parameters that are accepted to the chain forms a new starting point for the next process, and the process is repeated for a sufficient number of steps until the required convergence is reached. Our MCMC code is



based on the publicly available package COSMOMC [52]. We give both marginalized and likelihood limits of the uncorrelated parameters  $\mathcal{W}_i$ . The likelihood limit defines the region of parameter space enclosing a fraction  $f$  of the points with the highest likelihood as the  $N$ -dimensional confidence region, where  $f$  defines the confidence limit [52]. The likelihood limit is very useful to assess the consistency with new data or theories. For comparison, we also fit the result by running the publicly available package WZBINNED [53] and the results are consistent with those by using the marginalized method.

We first fit the parameters  $\boldsymbol{\theta}$  in the model by using the combined SnIa+BAO II data, i.e., we calculate  $\chi^2(\boldsymbol{\theta}) = [A(\boldsymbol{\theta}) - 0.469(0.96/0.98)^{-0.35}]^2/0.017^2 + \chi_{sn}^2(\boldsymbol{\theta}, H_0^n)$ . By fitting the piecewise constant model to the data, we get  $\chi^2 = 459.2$ , the marginalized  $1\sigma$  estimate  $\Omega_{m0} = 0.285_{-0.011}^{+0.034}$ , and the uncorrelated binned estimates of the equation of state parameters  $\mathcal{W}_i$  are shown in Fig. 2. We see that the results marginalizing over  $H_0^n$  analytically are the same as those with  $H_0$  marginalized numerically. In other words, we can trust the result using the method of analytically marginalizing over  $H_0^n$  with a flat prior. From Fig. 2, it is clear that the likelihood limits are larger than the marginalized limits, especially for the parameters  $\mathcal{W}_3$  and  $\mathcal{W}_4$ . If we take the likelihood limits, then the cosmological constant is consistent with the data even at  $1\sigma$  level. However, the cosmological constant is not consistent with the data at  $1\sigma$  level if we take the marginalized limits. Although the likelihood limits are useful information for the full MCMC sample, in the following, we quote the results obtained with marginalized limits. If we fit the flat  $\Lambda$ CDM model to the combined SnIa+BAO II data, we get  $\chi^2 = 466.4$  and  $\Omega_{m0} = 0.286 \pm 0.017$ . If we fit the flat CPL model to the data, we get  $\chi^2 = 466.2$ , and the marginalized  $1\sigma$  constraints are  $\Omega_{m0} = 0.288_{-0.016}^{+0.041}$ ,  $w_0 = -0.90_{-0.16}^{+0.30}$ , and  $w_a = -0.6_{-2.3}^{+1.1}$ . In Fig. 3, we show the marginalized probabilities of the parameters  $\mathcal{W}_i$ .

Now we add the BAO and WMAP5 data to the SnIa data. The parameters  $\boldsymbol{\theta}$  in the models are determined by minimizing  $\chi^2(\boldsymbol{\theta}, \Omega_b h^2, h) = \chi_{sn}^2 + \chi_{bao}^2 + \chi_{cmb}^2$ , here  $h = H_0/100$ . To use the BAO measurement (hereafter BAO III) from the SDSS data, we define [40]

$$\chi_{bao}^2(\boldsymbol{\theta}, \Omega_b h^2, h) = \left( \frac{r_s(z_d)/D_V(z=0.2) - 0.198}{0.0058} \right)^2 + \left( \frac{r_s(z_d)/D_V(z=0.35) - 0.1094}{0.0033} \right)^2, \quad (13)$$

where the redshift  $z_d$  is fitted with the formulae [54]

$$z_d = \frac{1291(\Omega_{m0} h^2)^{0.251}}{1 + 0.659(\Omega_{m0} h^2)^{0.828}} [1 + b_1(\Omega_b h^2)^{b_2}], \quad (14)$$

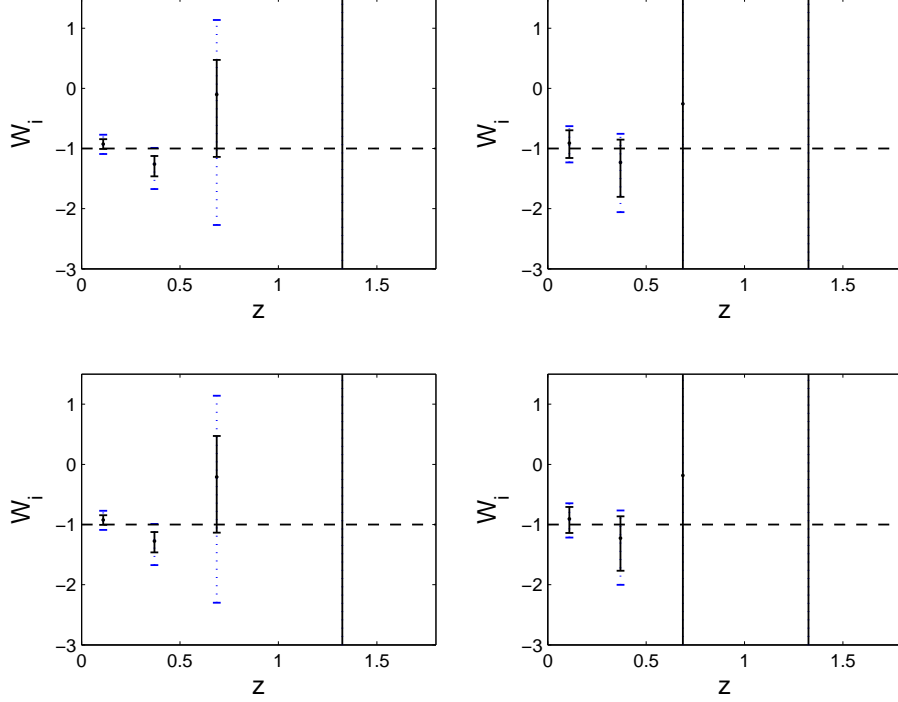


FIG. 2: The  $1\sigma$  and  $2\sigma$  estimates of the four uncorrelated parameters  $\mathcal{W}_i$  using the SnIa+BAO II data. The parameter  $\mathcal{W}_4$  is not well constrained. The error bars show  $1\sigma$  and  $2\sigma$  uncertainties with black solid lines and blue dotted lines, respectively. The top panels show the results by treating the nuisance parameter  $H_0^n$  as a free parameter, and the bottom panels show the results with  $H_0^n$  being analytically marginalized. The results in the left panels are the marginalized limits, while the results in the right panels are the likelihood limits.

$$b_1 = 0.313(\Omega_{m0}h^2)^{-0.419}[1 + 0.607(\Omega_{m0}h^2)^{0.674}], \quad b_2 = 0.238(\Omega_{m0}h^2)^{0.223}, \quad (15)$$

and the comoving sound horizon is

$$r_s(z) = \int_z^\infty \frac{dx}{c_s(x)E(x)}, \quad (16)$$

where the sound speed  $c_s(z) = 1/\sqrt{3[1 + \bar{R}_b/(1+z)]}$ , and  $\bar{R}_b = 315000\Omega_b h^2(2.726/2.7)^{-4}$ .

To implement the WMAP5 data, we need to add three fitting parameters  $R$ ,  $l_a$  and  $z_*$ , so  $\chi_{cmb}^2(\boldsymbol{\theta}, \Omega_b h^2, h) = \Delta x_i \text{Cov}^{-1}(x_i, x_j) \Delta x_j$ , where  $x_i = (R, l_a, z_*)$  denote the three parameters for WMAP5 data,  $\Delta x_i = x_i - x_i^{obs}$  and  $\text{Cov}(x_i, x_j)$  is the covariance matrix for the three parameters [43]. The acoustic scale  $l_A$  is

$$l_A = \frac{\pi d_L(z_*)}{(1+z_*)r_s(z_*)}, \quad (17)$$

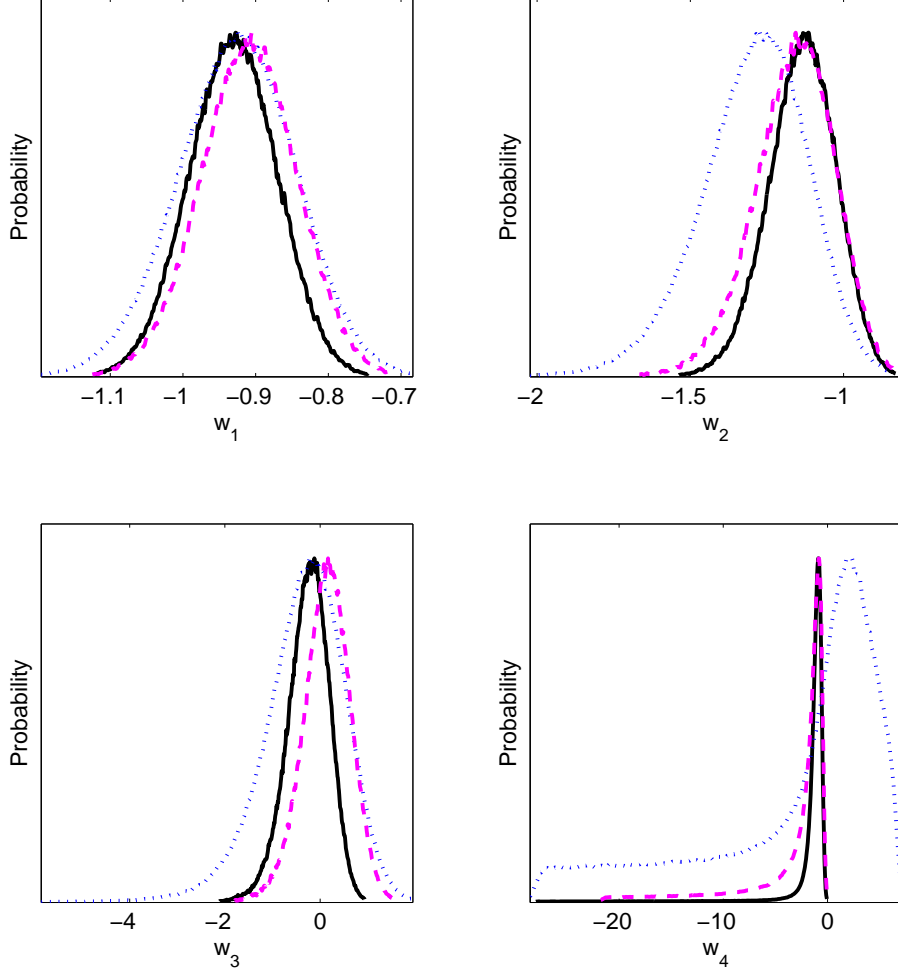


FIG. 3: The marginalized probabilities of the four equation of state parameters  $\mathcal{W}_i$ . The dotted lines are the results using SnIa+BAO II data only, the dashed lines are the results using the combined SnIa, BAO III and WMAP5 data, and the solid lines are the results using SnIa+BAO III+WMAP5+ $H(z)$  data. The nuisance parameter  $H_0^n$  in the SnIa is analytically marginalized over.

where the redshift  $z_*$  is given by [55]

$$z_* = 1048[1 + 0.00124(\Omega_b h^2)^{-0.738}][1 + g_1(\Omega_{m0} h^2)^{g_2}] = 1090.04 \pm 0.93, \quad (18)$$

$$g_1 = \frac{0.0783(\Omega_b h^2)^{-0.238}}{1 + 39.5(\Omega_b h^2)^{0.763}}, \quad g_2 = \frac{0.560}{1 + 21.1(\Omega_b h^2)^{1.81}}. \quad (19)$$

The shift parameter [43]

$$R(\boldsymbol{\theta}, \Omega_b h^2, h) = \sqrt{\Omega_{m0}} \int_0^{z_*} \frac{dz}{E(z)} = 1.710 \pm 0.019, \quad (20)$$

When we add the BAO III and WMAP5 data, we add two more parameters  $\Omega_b h^2$  and the Hubble constant  $H_0 = 100h$ . Because the normalization of the luminosity distance-redshift relation is unknown, the nuisance parameter  $H_0^n$  in the SnIa data is not the observed Hubble constant, and it is different from that in the BAO III and WMAP5 data. By fitting the data to the model, we find that the nuisance parameter  $H_0^n$  is around 65 km/s/Mpc in the Constitution data, while the Hubble constant  $H_0$  is around 72 km/s/Mpc. Therefore, we should treat the nuisance parameter  $H_0^n$  in the SnIa data differently from the Hubble constant  $H_0$  in other observational data, and we should include both  $H_0^n$  and  $H_0$  ( $h$ ) in the data fitting. We analytically marginalize over the nuisance parameter  $H_0^n$  in the SnIa data as explained in [27]. If we treat the nuisance parameter  $H_0^n$  as the Hubble constant, we get  $\chi^2 = 465.9$ , and the uncorrelated estimates of  $\mathcal{W}_i$  are shown in the top panels of Fig. 4. If the nuisance parameter  $H_0^n$  in the SnIa data is marginalized analytically, we get  $\chi^2 = 462.3$ ,  $\Omega_{m0} = 0.283_{-0.011}^{+0.020}$ , and the uncorrelated estimates of  $\mathcal{W}_i$  are shown in the bottom panels of Fig. 4. By adding the BAO III and WMAP5 data, we add 4 more data points, and  $\chi^2$  increases 3.1. With the help of the BAO III and WMAP5 data, the constraint on the equation of state parameters  $\mathcal{W}_i$  is improved, especially for  $\mathcal{W}_3$  and  $\mathcal{W}_4$ . This point is also clear from the marginalized probabilities shown in Fig. 3. From Fig. 4, we see that the results are different if the nuisance parameter  $H_0^n$  is treated differently. As explained above and in [27], we should treat the nuisance parameter  $H_0^n$  in the SnIa data differently, so we analytically marginalize over  $H_0^n$  with a flat prior when fitting the SnIa data. Again, we see that the marginalized limits give tighter constraints on the parameters than the likelihood limits do, so we quote the result in the bottom left panel as the fitting result.

Finally, we add the data of the Hubble parameter  $H(z)$  at nine different redshifts from the differential ages of passively evolving galaxies obtained in [46] and the three more recent data  $H(z = 0.24) = 79.69 \pm 2.32$ ,  $H(z = 0.34) = 83.8 \pm 2.96$ , and  $H(z = 0.43) = 86.45 \pm 3.27$  by taking the BAO scale as a standard ruler in the radial direction [47]. To use these 12  $H(z)$  data, we define

$$\chi_h^2(\boldsymbol{\theta}, h) = \sum_{i=1}^{12} \frac{[H_{obs}(z_i) - H(z_i)]^2}{\sigma_{hi}^2}, \quad (21)$$

where  $\sigma_{hi}$  is the  $1\sigma$  uncertainty in the  $H(z)$  data. We also add the prior  $H_0 = 74.2 \pm 3.6$  km/s/Mpc determined from the observations with the Hubble Space Telescope by Riess *et al.* [48]. Now we have  $\chi^2(\boldsymbol{\theta}, \Omega_b h^2, h) = \chi_{sn}^2 + \chi_{bao}^2 + \chi_{cmb}^2 + \chi_h^2$ .

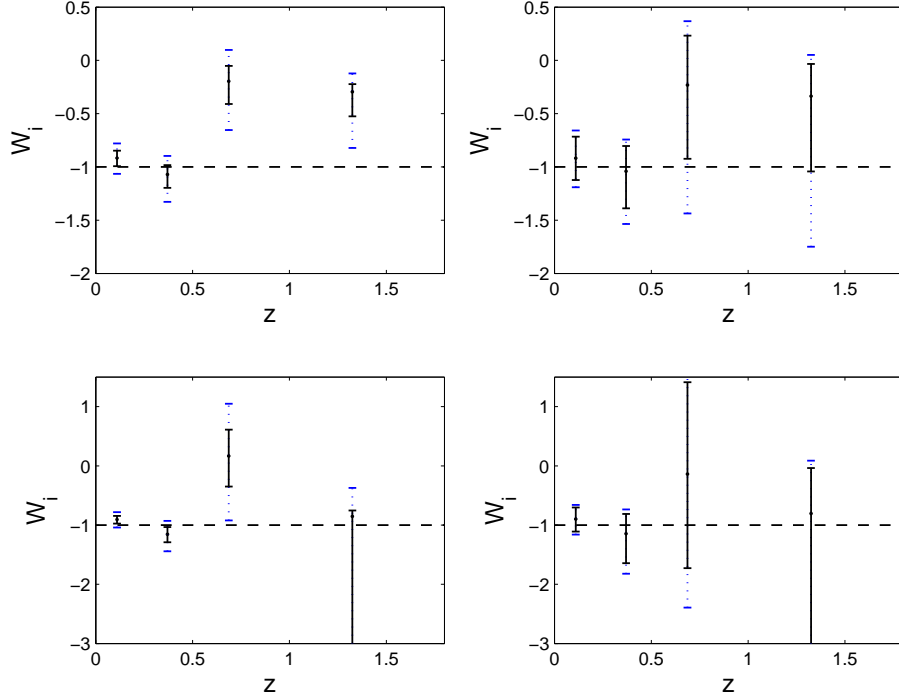


FIG. 4: Same as Fig. 2 except that we use SnIa + BAO III + WMAP5 data here.

If we treat the nuisance parameter  $H_0^n$  as the Hubble constant, we get  $\chi^2 = 500.5$ , and the uncorrelated estimates of  $\mathcal{W}_i$  are shown in the top panels of Fig. 5. If the nuisance parameter  $H_0^n$  in the SnIa data is marginalized analytically, we get  $\chi^2 = 476.8$ ,  $\Omega_{m0} = 0.271_{-0.006}^{+0.021}$ , and the uncorrelated estimates of  $\mathcal{W}_i$  are shown in the bottom panels of Fig. 5. By adding the  $H(z)$  data, we add 13 data points, and  $\chi^2$  increases 14.5. As explained above, due to the difference between the nuisance parameter  $H_0^n$  in the SnIa data and the Hubble constant  $H_0$ , we get much larger value of  $\chi^2$  if we treat the nuisance parameter  $H_0^n$  in the SnIa data as the Hubble constant, so we should use the results in the bottom left panel. If we fit the data to the flat  $\Lambda$ CDM model, we get  $\chi^2 = 483.0$  and  $\Omega_{m0} = 0.272 \pm 0.011$ . If we fit the data to the flat CPL model, we get  $\chi^2 = 482.5$ ,  $\Omega_{m0} = 0.269_{-0.008}^{+0.017}$ ,  $w_0 = -0.97_{-0.07}^{+0.12}$ , and  $w_a = 0.03_{-0.75}^{+0.26}$ . These results suggest that the CPL model is consistent with  $\Lambda$ CDM model at  $1\sigma$  level, and  $\Lambda$ CDM model is consistent with the piecewise constant parametrization at  $2\sigma$  level.

The marginalized probabilities of the parameters  $\mathcal{W}_i$  are shown in Fig. 3. From Figs. 3 and 5, we see that the addition of the  $H(z)$  data improves the constraint on  $\mathcal{W}_4$  by 70%. This suggests that the equation of state parameter at high redshift will be better constrained

with high quality data of  $H(z)$  in the future.

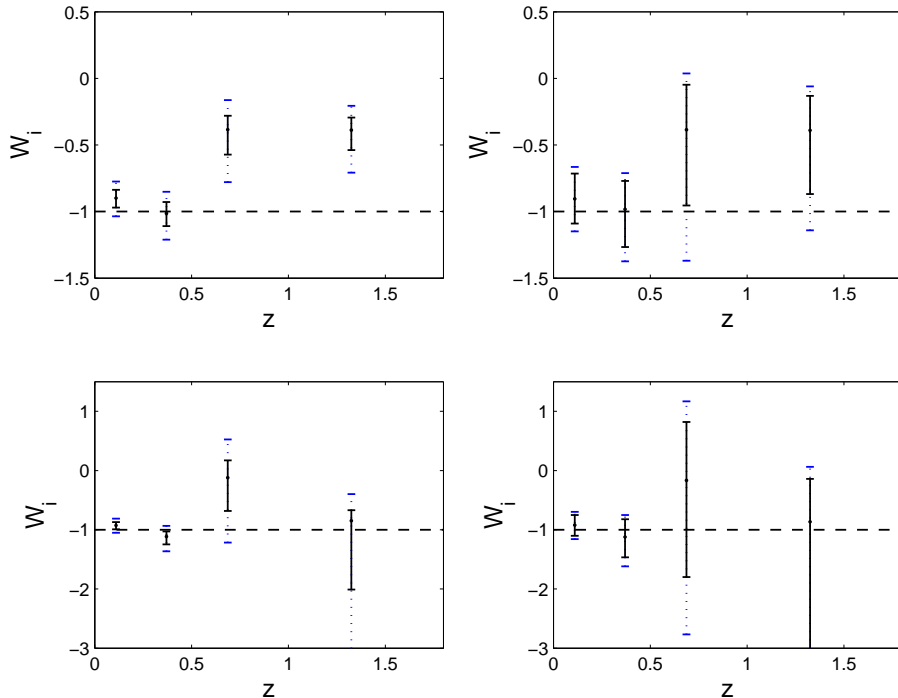


FIG. 5: Same as Fig. 2, except that we use the combined SnIa, BAO III, WMAP5 and  $H(z)$  data here.

#### IV. CONCLUSIONS

Fitting the combined SnIa and the BAO distance ratio (BAO I) data to the CPL model, we find that  $\chi^2 = 462.44$ , and the joint  $1\sigma$  constraints  $\Omega_{m0} = 0.45^{+0.07}_{-0.11}$ ,  $w_0 = -0.13^{+1.26}_{-0.95}$  and  $w_a = -12.2^{+10.3}_{-15.3}$ . Fitting the combined SnIa and the BAO A (BAO II) data to the CPL model, we find that  $\chi^2 = 466.18$ , and the joint  $1\sigma$  constraints  $\Omega_{m0} = 0.29^{+0.05}_{-0.04}$ ,  $w_0 = -0.90^{+0.46}_{-0.37}$  and  $w_a = -0.6^{+2.5}_{-3.5}$ . While the results obtained with the BAO I data are not consistent with the  $\Lambda$ CDM model at more than  $1\sigma$  level [35], the results obtained with the BAO II data are consistent with the  $\Lambda$ CDM model at  $1\sigma$  level (see Fig. 1), and the constraints are tighter. So different BAO data give different results. The inconsistency lies mainly on the larger value of  $\Omega_{m0}$  obtained with the BAO I data.

To constrain the property of dark energy using the observational data, we need to apply model independent method. The piecewise constant parametrization of the equation

of state parameter  $w(z)$  of dark energy is somewhat model independent, we used the current observational data to study the property of dark energy with this model independent parametrization. Since the normalization of the luminosity distance-redshift relation is arbitrary, the nuisance parameter  $H_0^n$  in the SnIa data is also arbitrary, and different from the observed Hubble constant  $H_0$ . We should treat it differently from the Hubble constant in other data, and we should include both  $H_0^n$  and  $H_0$  ( $h$ ) in the data fitting. Otherwise, we may get wrong conclusions. If we treat the nuisance parameter  $H_0^n$  in the SnIa data as the observed Hubble constant, then we may conclude that the flat  $\Lambda$ CDM model is incompatible with the combined SnIa, BAO III and WMAP5 data or the combined SnIa, BAO III, WMAP5 and  $H(z)$  data. However, by marginalizing over the nuisance parameter  $H_0^n$  analytically in computing  $\chi_{sn}^2$ , the flat  $\Lambda$ CDM model is consistent with the current observation at  $2\sigma$  level.

By fitting the combined SnIa, BAO III, WMAP5 and  $H(z)$  data to the flat  $\Lambda$ CDM model, we get  $\chi^2 = 483.0$  and  $\Omega_{m0} = 0.272 \pm 0.011$ . If we fit the data to the flat CPL model, we get  $\chi^2 = 482.5$ , and the marginalized  $1\sigma$  constraints  $\Omega_{m0} = 0.269_{-0.008}^{+0.017}$ ,  $w_0 = -0.97_{-0.07}^{+0.12}$ , and  $w_a = 0.03_{-0.75}^{+0.26}$ . If we fit the model with piecewise constant parametrization to the data, we get  $\chi^2 = 476.8$ , and the marginalized  $1\sigma$  constraints  $\Omega_{m0} = 0.271_{-0.006}^{+0.021}$ ,  $\mathcal{W}_1 = -0.93 \pm 0.06$ ,  $\mathcal{W}_2 = -1.13_{-0.12}^{+0.10}$ ,  $\mathcal{W}_3 = -0.12_{-0.56}^{+0.29}$ , and  $\mathcal{W}_4 = -0.85_{-1.16}^{+0.18}$ .

By adding the  $H(z)$  data to the SnIa, BAO III and WMAP5 data, the constraint on the parameters is greatly improved, especially for the equation of state parameter at high redshift where the number of SnIa data is small. The result suggests that the equation of state parameter at high redshift will be better constrained with high quality data of  $H(z)$  in the future.

## Acknowledgments

YG and ZZ wish to acknowledge the hospitality of the KITPC under their program ‘‘Connecting Fundamental Theory with Cosmological Observations’’ during which this project was initiated. YG thanks A. Cooray, D. Sarkar, A. Riess and B. Gold for the fruitful discussion on the MCMC code. This work was partially supported by the Chinese Academy of Sciences under grant No. KJCX3-SYW-N2, the National Natural Science Foundation of China key project under grant Nos. 10533010 and 10935013, and the Ministry of Science

and Technology of China national basic research Program (973 Program) under grant Nos. 2007CB815401 and 2010CB833004. ZZ acknowledges the supported by the National Natural Science Foundation of China under the Distinguished Young Scholar Grant No. 10825313. YG acknowledges the support by the Natural Science Foundation Project of CQ CSTC under grant No. 2009BA4050.

---

- [1] A.G. Riess *et al.*, *Astron. J.* **116**, 1009 (1998).
- [2] S. Perlmutter *et al.*, *Astrophys. J.* **517**, 565 (1999).
- [3] G. Dvali, G. Gabadadze and M. Porrati, *Phys. Lett. B* **485**, 208 (2000).
- [4] S.M. Carroll, V. Duvvuri, M. Trodden, M.S. Turner, *Phys. Rev. D* **70**, 043528 (2004).
- [5] T. Chiba, *Phys. Lett. B* **575**, 1 (2003).
- [6] S. Nojiri, S.D. Odintsov, *Phys. Rev. D* **68**, 123512 (2003).
- [7] C.G. Shao, R.G. Cai, B. Wang, R.K. Su, *Phys. Lett. B* **633**, 164 (2006).
- [8] S. Capozziello, *Int. J. Mod. Phys. D* **11**, 483 (2002).
- [9] S. A. Appleby and R. A. Battye, *Phys. Lett. B* **654**, 7 (2007).
- [10] S. Nojiri, S.D. Odintsov, *Int. J. Geom. Meth. Mod. Phys.* **4**, 115 (2007).
- [11] A. A. Starobinsky, *JETP Lett.* **86**, 157 (2007).
- [12] W. Hu, I. Sawicki, *Phys. Rev. D* **76**, 064004 (2007).
- [13] S. Nojiri, S.D. Odintsov, *Problems of Modern Theoretical Physics*, P. 266-285, 2008.
- [14] P. Astier, *Phys. Lett. B* **500**, 8 (2001).
- [15] D. Huterer and M.S. Turner, *Phys. Rev. D* **64**, 123527 (2001).
- [16] J. Weller and A. Albrecht, *Phys. Rev. Lett.* **86**, 1939 (2001); D. Huterer and G. Starkman, *ibid.* **90**, 031301 (2003).
- [17] G. Efstathiou, *Mon. Not. Roy. Astron. Soc.* **310**, 842 (1999); P.S. Corasaniti and E.J. Copeland, *Phys. Rev. D* **67**, 063521 (2003).
- [18] U. Alam, V. Sahni, T.D. Saini and A.A. Starobinsky, *Mon. Not. Roy. Astron. Soc.* **354**, 275 (2004).
- [19] H.K. Jassal, J.S. Bagla and T. Padmanabhan, *Mon. Not. Roy. Astron. Soc.* **356**, L11 (2005).
- [20] R.A. Daly and S.G. Djorgovski, *Astrophys. J.* **597**, 9 (2003); R.A. Daly and S.G. Djorgovski, *ibid.* **612**, 652 (2004).



- [21] C. Wetterich, Phys. Lett. B **594**, 17 (2004).
- [22] D. Huterer and A. Cooray, Phys. Rev. D **71**, 023506 (2005).
- [23] Y.G. Gong, Class. Quantum Grav. **22**, 2121 (2005); Y.G. Gong, Int. J. Mod. Phys. D **14**, 599 (2005); Y.G. Gong and A. Wang, Phys. Lett. B **652**, 63 (2007); Y.G. Gong, A. Wang, Q. Wu and Y.Z. Zhang, J. Cosmol. Astropart. Phys. **01** (2007) 024.
- [24] Y.G. Gong and Y.Z. Zhang, Phys. Rev. D **72**, 043518 (2005); M. Manera and D.F. Mota, Mon. Not. Roy. Astron. Soc. **371**, 1373 (2006); S. Basilakos, M. PLionis and J. Sola, arXiv: 0907.4555.
- [25] Y.G. Gong and A. Wang, Phys. Rev. D **73**, 083506 (2006); Y.G. Gong and A. Wang, Phys. Rev. D **75**, 043520 (2007); Y.G. Gong, Phys. Rev. D **78**, 123010 (2008); Y.G. Gong, M. Ishak and A. Wang, Phys. Rev. D **80**, 023002 (2009).
- [26] M. Goliath et al., Astron. and Astrophys. **380**, 6 (2001).
- [27] Y.G. Gong, Q. Wu and A. Wang, Astrophys. J. **681**, 27 (2008).
- [28] M. Ishak, Foundations of Phys. J. **37**, 1470 (2007).
- [29] A. Upadhye, M. Ishak and P.J. Steinhardt, Phys. Rev. D **72**, 063501 (2005).
- [30] V. Sahni, A. Shafieloo and A.A. Starobinsky, Phys. Rev. D **78**, 103502 (2008).
- [31] C. Zunckel and C. Clarkson, Phys. Rev. Lett. **101**, 181301 (2008).
- [32] S. Qi, F.-Y. Wang and T. Lu, Astron. Astrophys. **483**, 49 (2008).
- [33] M. Chevallier and D. Polarski, Int. J. Mod. Phys. **10**, 213 (2001).
- [34] E.V. Linder, Phys. Rev. Lett. **90**, 091301 (2003).
- [35] A. Shafieloo, V. Sahni and A.A. Starobinsky, Phys. Rev. D **80**, 101301 (2009).
- [36] S. Qi, T. Lu and F.-Y. Wang, Mont. Not. R. Astron. Soc. **398**, L78 (2009).
- [37] Q.G. Huang, M. Li, X.D. Li and S. Wang, Phys. Rev. D **80**, 083515 (2009).
- [38] G.B. Zhao and X.M. Zhang, arXiv: 0908.1568.
- [39] M. Hicken *et al.*, Astrophys. J. **700**, 1097 (2009).
- [40] W.J. Percival *et al.*, Mont. Not. R. Astron. Soc. **381**, 1053 (2007).
- [41] M. Kowalski *et al.*, Astrophys. J. **686**, 749 (2008).
- [42] D.J. Eisenstein *et al.*, Astrophys. J. **633**, 560 (2005).
- [43] E. Komatsu *et al.*, Astrophys. J. Suppl. **180**, 330 (2009).
- [44] P. Serra *et al.*, arXiv: 0908.3186.
- [45] B.A. Reid, arXiv: 0907.1659; W.J. Percival *et al.*, arXiv: 0907.1660.

- [46] J. Simon, L. Verde and R. Jimenez, *Phys. Rev. D* **71**, 123001 (2005).
- [47] E. Gaztañaga, A. Cabré and L. Hui, arXiv: 0807.3551.
- [48] Riess *et al.*, *Astrophys. J.* **699**, 539 (2009).
- [49] P. Astier *et al.*, *Astron. and Astrophys.* **447**, 31 (2006).
- [50] A.G. Riess *et al.*, *Astrophys. J.* **659**, 98 (2007).
- [51] W.M. Wood-Vasey *et al.*, *Astrophys. J.* **666**, 694 (2007); T.M. Davis *et al.*, *Astrophys. J.* **666**, 716 (2007).
- [52] A. Lewis and S. Bridle, *Phys. Rev. D* **66** (2002) 103511.
- [53] D. Sarkar *et al.*, *Phys. Rev. Lett.* **100**, 241302 (2008).
- [54] D.J. Eisenstein and W. Hu, *Astrophys. J.* **496**, 605 (1998).
- [55] W. Hu and N. Sugiyama, *Astrophys. J.* **471**, 542 (1996).